

“The Covid-19 virus double pathogenic mechanism. A new perspective”.

Author: Carlo Brogna* M.D.

Abstract.

Acetylcholine (ACh) is the best one characterized neurotransmitter. Its central roles in the cholinergic areas and central nervous system (CNS) and peripheral (PNS) synapses are well known. It was the first molecule identified as a neurotransmitter and appears to be phylogenetically the oldest one signaling molecules. ACh was detected in bacteria, protozoa, fungi, algae and primitive plants, indicating that the cholinergic system was widely distributed in living organisms before its appearance in the nervous system. The autonomous nervous system (ANS) is an integral part animal kingdom history. It determines fight-escape reactions as well as outlining the vital and cognitive functions bio-organization rhythms. The virus (Covid-19) extraneous effects acting on it could help to better understand its functions. The Blast results show some factors like protein that can be implicated such as *bungaro-toxins*, *phospholipase A2* and *the similar prothrombin activator protein*. A positive correlation with different toxins is obtained and the Covid-19 double pathogenic mechanism theory is proposed. The process allows us to outline the possibility about toxic-like factors presence.

Key words: Covid-19; Blastn; toxins protein; ACh; aChE; BuChE; CBP; Zero Point; bungaro-toxins, phospholipase A2; similar prothrombin activator protein.

Introduction.

Beta-coronaviruses are capsuled and have a single RNA filament with a positive sense, ranging in size from 26 to 32 kilobas. The genome encodes for structural, non-structural and ancillary proteins. In 2002, severe acute coronavirus syndrome (SARS-CoV) emerged in China. The SARS-CoV outbreak lasted 8 months and led to 8,098 confirmed human cases worldwide, 774 (9.5%) Fatal. About 10 years later, another highly pathogenic human coronavirus, Middle East Respiratory Syndrome (MERS-CoV), appeared in the Saudi Arabia Kingdom affecting 2,260 cases in 27 countries and 803 were fatal. Many human and animal coronaviruses appear to originate from a bat species variety. Sequencing with new-generation techniques, there are about 200 new coronaviruses. SarS-CoV studies suggested Himalayan palm civets and raccoon as the most likely

hosts responsible for human transmission. The bats role has been hypothesized later. Dromedary camels are a natural host and tank for MERS-CoV, but primary MERS-CoV cases have had no contact history with camels or infected individuals. HCoV-NL63 was first identified in 2004 in a pediatric patient with bronchiolitis and since then it has been learned that the virus causes about 1-9% common colds each year and has been circulating in humans for centuries. Although viruses like to HCoV-NL63 have been identified in bats, they have fairly distant sequences, *suggesting a possible intermediate host*. HCoV-229E, which causes the common cold, appears to have its origins even in bat species. HCoV-229E-related viruses have been found in hipposider bats in Kenya and Ghana. In 2007, an alpha-coronavirus was identified in a respiratory disease epidemic in the United States alpacas. *Genomic changes Evidence in the HCoV-229E evolution, between bat and alpacas* and subsequently between alpacas and human evolution has been identified. *Bats remain the main evolutionary reservoirs and CoV diversity ecological drivers* (1). SARS genomic sequences are related to CoVid-19 and other animal species. The epidemic virus initial stages in Wuhan, December 2019, are probably related to the fish market (2). Some studies suggest the *bat as a potential host* (3). The SARS-CoV-2 genomic sequence is 96.2% identical to the CoVRaTG13 sequence, as well as having a 79.5% genomic identity with SARS-CoV. The bat is suspected as a natural host and SARSCoV-2 may have been transmitted to humans by an unknown intermediate *host*. It is found that SARS-CoV-2 uses the angiotensin 2 *conversion enzyme receptor* as well as SARS-CoV and establishes an avid receptor *link* with pneumocytes cells (4,12). *Ace2* pneumocyte regulates *both cross-species and transmission between humans* (11). The coronavirus surface S-glycoprotein virion binds to the ACE2 receptor (13,14,15,16,). Ace2-receptor adherence efficiency is 10 to 20 times higher than SARS-CoV (14,15,16). The protein sequences alignment and phylogenetic analysis, considering that similar residues ACE receptor have been observed in many species, suggest more alternative intermediate hosts possibilities, such as turtles, pangolin and snakes. The SARS-CoV-2 interhuman transmission takes place mainly among family members, including relatives and friends (5,6). The Wuhan-Hu-1 Coronavirus (WHCV) complete genome, a SARSCoV-2 strain, is 29.9 kb (6) while SARS-CoV and MERS-CoV has 27.9 kb and 30.1 kb positive RNA genomes, respectively (7). An open reading frames (ORF) variable number (six to eleven) the SARSCoV-2 genome contains. The $\frac{2}{3}$ RNA viral

genome, the first ORF (ORF1a/b), translates two polyproteins, pp1a and pp1ab, and encodes 16 non-structural proteins (NSPs) while the remaining ORFs encode *ancillary* and structural proteins. The remaining part encodes essential structural proteins (glycoprotein spike (S), small envelope protein (E), matrix protein (M) and nucleocapsid protein (N)) and several ancillary *proteins* who interfere with the human immune response (8,9). There are genomic and phylogenetic similarities with SARS-CoV in the S-glycoprotein gene and receptor-binding (RBD) domain, which indicates human direct transmission capacity. Mutations in NSP2 and NSP3 plays a role in the infectious capacity and SARS-CoV-2 differentiation mechanism (9). The viral RNA receptor gene inducible retinoic acid I (RIG-I), a differentiated melanoma cytosolic receptor associated with gene 5 (MDA5) and the cyclic nucleotide-transferase synthesizer GMP-AMP (cGAS) are responsible for the RNA and DNA recognition in cytoplasm. These complexes lead to the nuclear factor-B transcription (NF-B) and the interferon factor 3 (IRF3) activation, and regulators the interferons type I (IFN-z) and pro-inflammatory cytokines, including IL-1, IL-2, IL-4, IL-7, IL-10, IL-12, IL-13, IL-17, GCSF, Macrophage Colony Stimulation Factor (MCSF), IP-10, MCP-1, MIP-1, Hepatocyte Growth Factor (HGF), IFN-z and TNF-z, production (17-18-19-20).

In Wuhan, the 73% patients infected (average age 49 years) were men, 32% had underlying conditions including diabetes (20%), hypertension (15%) cardiovascular disease (15%). The most common symptoms onset were: fever (98%), cough (76%) and myalgia or fatigue (44%). Less common symptoms: sputum (28%), headaches (8%), hemoptysis (5%) diarrhea (3%). The average time from the first symptom to breathlessness was 5 days, to the hospitalization 7 days and to ARDS 8 days. Lymphopenia was present in the 63%. All patients had interstitial pneumonia with abnormal chest CT results. Complications included: acute respiratory distress syndrome (29%), RNA grow (15%), acute heart damage (12%), secondary infection (10%). Most patients received antiviral therapy (oseltamivir, 89.9%) and many received antibacterial therapy (moxifloxacin, 64.4%; ceftriaxone, 24.6%; azithromycin, 18.1% and glucocorticoid therapy, 44.9%). Between 26.1% and 32% patients needed intensive care due to complications, including acute respiratory distress syndrome (61.1%), arrhythmia (44.4%) shock (30.6%). The latter had higher plasma levels of IL2, IL7, IL10, GSCF, IP10, MCP1, MIP1A, and TNF. Patients treated in intensive care, compared

to patients not treated in intensive care, were older (median age, 66 years vs. 51 years), and 72.2% had underlying comorbidity (23.24).

The Guidelines (VI^o edition) recommended antivirals, including IFN- γ , lopinavir/ritonavir, ribavirin, chloroquine phosphate (30). As in the past, convalescent blood products (CBP) infusion has been practiced in Wuhan. They can derive from whole blood or plasma (convalescent whole blood, convalescent plasma or convalescent serum, healed pooled human immunoglobulin (Ig) a and immunized patient, high-title human Ig, polyclonal or monoclonal antibodies), like Ebola, Sars, Mers protocols (22). *Wei Ji et al. 2020 suggest that 2019-nCoV has a very similar bat coronaviruses genetic information and that there is a more similar sequence to snake bias; two snakes' types - the Bungarus multicinctus (multi-band krait) and the Naja atra (Chinese cobra).*

Materials and Methods.

Collected and analyzed the data, published from January 2020 to 28.03.2020, *10 safe and certain axioms are postulated (Table 1) and the absurd hypothesis: "The covid-19 is not just a virus is formulated.* This analysis is called as "*Reductio Ad Absurdum*".

Axioms (Table 1):

1.	No study has denied an intermediate host.
2.	The Covid-19 virus is respiratory.
3.	The Covid-19 virus has an interhuman spread.
4.	There isn't the same out-come in covid-19 patients about age
5.	There isn't the same out-come in covid-19 patients about previous health status.
6.	There isn't the same out-come in covid-19 patients about gender.
7.	There is contracting Covid-19 greater individuals' group risk. (Health workers- patients with comorbidity- elderly and others for unknown reasons).
8.	the covid-19 cans be also contracted by direct contact.
9.	No study <i>verified</i> other unknown covid-19 properties and/or proteins acquired by the intermediate host.
10.	No study has <i>denied</i> the traits and/or characteristics and/or proteins (or RNA genomic sequences, Micro Rna, enzymes or molecules) acquisition possibility by the intermediate host.

The Questions to Be Met.

1. *Could the Covid-19 virus have acquired, in its genomic set, sequences that transcribe factors (micro-Rna? Enzymes? Proteins? Toxins? else?) like those in the intermediate host? A: Unknown? Cross species genomic recombination? (21)*

2. *Is there another laboratory data besides the useful nasal or oral-pharyngeal swab at any way? A: Unknown*

3. *If the absurd hypothesis were true, would the treatments and therapies be enough?*

The analysis.

A genomic sequence *blast-alignments* series were performed to verify the analyzed data match and the "genesis", the "zero point". Alignments were made through the BLAST-algorithm (blastn.ncbi.nlm.nih.gov) and were practiced between the Covid19 (id. NC_045512.2.), the pangolin ("Manis pentadactyla") and the snakes Bungarus multicinctus, fasciatus, the Naja Atra. The snakes produce toxins and are suggested by *Wej Ji as intermediate host*. The acid secreted by the pangolin's glands (KN005617.1, blast-n fig. 5) had no use in medicine while snake toxins were particularly studied, sequenced, recombined, reproduced and used for analysis cholinergic receptor mechanisms, as precursors to many drugs including Captopril and congeners, such as antithrombotic drugs. The toxins originated from early positive results for a significant correlation between these molecules and the Covid-19 genome, is defined by the match with a low e-value and a high identity rate.

The best toxins' correlations are:

B. multicinctus peptide 1 similar to neurotoxin (NL1) (X64593.1), Query cover 32%, e-value 0.5, 100% identity percentage (Figure 1A);

Cardiotoxin VII Naja atra (id. U42584.1), Q.C. 26%, e-v. 0.048, for. Id. 100% (fig 1B);

Bungarotoxin (V31) Bungarus multicinctus alpha- (id. Y17057.1) Q.C 31%, e-v.0.092 for. Id 89.47% (fig 1C);

Clone pGEMT-BMNTL4 Bungarus multicinctus mRNA (id. AJ007764.1) Q.C. 33%, e-v 0.092 for. Id. 100.00% (fig 2.D);

Alpha- bungarus3ftx Type II (id. CAB51841.1) Query 32%, e-v. 0.14, per.Id. 93.75% (Figure 2.E);

Beta bungaratoxin B2a chain Bungarus ca. (id. AAL30066.1) Q.C. 54%, e-v. 0.19, per.id. 93.33% (fig 3 F);

Prothrombin activator Tropidechis ca. (id. DQ533832.1) Q.C. 32%, e-v. 0.003, per.id. 100% (fig 3.G);

PLA2 gene for phosp. Laticauda la. (id. AB062441.1) Q.C. 16%, e-v. 0.2, per.id. 89.47% (fig 3.H);

Ophiophagus precursor gene hannah Ohanin (king naja), (DQ103590.1) Q.C. 16%, e-v.0.056, id.100% (fig 4.);

The deductive/inductive process.

Neurotoxins are divided into two categories: short chain (60-62 amino acids, four-disulfide bonds) and long chain (66-74 amino acids or more and with five-disulfide bonds). The long-chain peptide binds with greater affinity to the alpha-7 nACh receptors, through the fifth disulfide bond (*neuronal k-bungarotoxin*) (28). The *three-finger toxins* (about 70 3FTxs: *cardiotoxic and neurotoxic*) family are 60-74 amino acid residues polypeptides composed. They show different functionality while have a preserved structure. A distinct structural feature is the unique fold, consisting of three rings (-stranded), which emerge from a hydrophobic globular core. The four or five disulfide bonds, obliged with some Cys, stabilized three-dimensional structure. Short rings length, conformations and amino acid residue variations are their distinct biological functions responsible (77). *Fasciculine*, with their loops and key amino-acids placed on the outside, creates a complex fasciculine-Ache (78). Toxic *A2 phospholysis* interacts with acetyl-choline nicotinic receptors (27.36). Almost all these toxins bind with high affinity to the acetylcholine nicotinic receptors (AChR) periphery (28). In some studies, alpha carbotoxin amino acids, Ala-28, Lys-35 and Cys-26-Cys-30 have been seen to selectively bind to alpha 7-AChR, while Lys-23 and Lys-49 bind exclusively to AChR Torpedo. Therefore, alpha-Cbtx binds to two AChR subtypes using both common and specific residues. *The link with toxins probably occurs in neuronal and muscular AChR homologous regions* (67,68). Probably, a small ring cycled, with a solid

disulfide bond and uniquely present in long-chain toxins, could serve as discriminating element, and a small toxin fold structural deviation can generate a unique discriminatory recognition for some receptor subtypes (69). The Three-finger toxins (3FTxs) block post-synaptic transmission through nicotinic receptors (nAARTr). The three-fingered toxin fold plasticity has evolved optimally to use different functional groups combinations, to generate a targets specificity panoply, to discern fine differences between nAChR subtypes. (33). Alpha-bungarotoxin binds to skeletal muscle nicotinic receptors, block neuromuscular transmission (29). Protamine and polylysine are even more potent than B. multicinctus cardiotoxin inhibiting cholinesterase (32,34). Some toxins have a basic phospholipase unit and possess anticoagulant properties; others induce the platelets aggregation; others instead inhibit it. Many “curare” toxins with three-fingered structure recognize a protein that binds to acetylcholine and block nicotinic receptors in skeletal muscles producing flaccid paralysis. Other toxins recognize acetylcholine receptors located on neurons. Cardiotoxins damage heart function; they depolarize numerous excitable cells membranes and are powerful cytotoxins. In total, toxins with three-finger structure exercise at least seven different functions. Certain snake poisons toxins don't belong to any of the two structural categories mentioned. Sarafotoxins are 21 amino acids vasoconstrictor peptides, with two disulfide bonds. Finally, the disintegrins possess the preserved sequence arginine-glycine-aspartic and inhibit the platelets aggregation and recognize proteins glycoprotein IIb/IIIa (70-75). Selectively bind the integrin receptors on platelets surface and other cells. Tirofiban and Eptifibatide are derived and used as antithrombotic agents (77). Protein toxins activate prothrombin, including Xa coagulation factor (FXa) (79). The Kunitz type inhibitor works inhibiting serine and proteases (e.g. plasmin, kallikrein, trypsin). It interferes with the coagulation cascade and fibrinolysis (76,77). In acute coronary syndrome there is a high chemokine CXCL12 and its CXCR4-CXCR7 receptor platelet surface expression and it influences prognosis (80).

Most toxins are, however, aChE inhibitors (37). Low aChE concentration is associated with mortality increased in patients with reduced left ventricular ejection fraction for any reason, and the mortality risk increases for all causes related to the aChE functionality (38). While the cholinesterase may be similar by gender and age, not so the erythrocytes cholinesterase activity may variable (39). The BuChE deficiency prevalence is highest among

European: the population has a partial deficiency *between* 3.4 and 4%. The most severe form prevalence is estimated at 1: 100,000. *BuChE deficiency has hereditary and non-hereditary causes*. The genetic defect, mutations in BCHE-Gen, is inherited in an autosomal recessive gene (*locus E1 in the chromosomal region 3q26.1-q26.2*). The acylation/catalytic site offers the Ser, His and Glu triad for aChE and Ser, his and Glu for the BuChE, suitable for inhibition. ACh substrates, as well as its inhibitors, can covalently bind to the active site following the attack on the substrate's carboxylic group by the hydroxyl anion Ser. The choline / cationic middle site within the aChE and BuChE site contains amino acids (Trp and Tyr in aChE, Trp and Wing in BuChE) that interact with the quaternary amino group within the ACh residue to optimally orient the molecule. The blocking site and, therefore, the substrate approach by the catalytic triad within the acylation/catalytic site will clearly reduce the aChE and/or BuChE ability to metabolize ACh and prolong its drug action (55,56,57,58,59,60,61,62,63,64).

In all *disorders associated with a cortical presynaptic cholinergic deficiency, reflected with a choline acetyl-transferase extensive loss* (Alzheimer's disease, Parkinson's disease and Down syndrome) there is a substantial nicotine binding nicotinic receptor reduction, in the bond (3h). In contrast, reductions both muscarinic subtypes (M1 and M2) are moderate in Alzheimer's disease while significantly increase (apparently not in relation to anti-cholinergic drug treatment) in Parkinson's disease and in cases with dementia but not in those without. (81).

A BuChE non-hereditary deficiency can occur in pregnancy, in newborns or in chronic infections, malnutrition, liver diseases and cancers, iron deficiency anemia and drugs such as cocaine, morphine, codeine, succinylcholine, OP poisoning" or from excess acetylcholinesterase inhibitors (Assumption for PD and AD) cases. Inhibit acetylcholinesterase (aChE) and increase the acetylcholine availability in cholinergic synapses, improves cholinergic transmission in the Alzheimer's disease (AD) pharmacological treatment. On the other hand, the *pneumonia cumulative incidence is 51.9 per 1000 cases, or 5.19%, in subjects over 65 years old, who are in therapy for dementia with cholinesterase inhibitor, galantamine, or rivastigmine* (35).

If cholinesterase doesn't increase within 48 hours by intoxication, they are associated with increased mortality due to excess inhibitors (43). They are measured *by the dibucaine and fluoride inhibition test*. The dibucaine

number represents the enzyme activity inhibition value in drug or toxins presence (41,42). The *S100B serum value* are higher in *mechanically ventilated patients* and serve to predict the need for more aggressive therapy during acute poisoning (42). The two closely homologous enzymes, acetylcholinesterase and butyryl cholinesterase (aChE and BuChE, respectively) are *useful as biomarkers in diseases associated with parasympathetic malfunction*. Blood cholinesterase measurements are an *easily quantifiable reading for changes in sympathetic/parasympathetic balance, and the changes implications are understood to be health and disease reading*. In our body, two classes of cholinesterase enzymes coexist and possess several *cholinergic and non-cholinergic functions, depending on their expression time, position and specific subtype form*. Although, aChE also predominates at the neuronal level, BuChE is widely localized and secreted by glial cells. Neurons possess BuChE rather than aChE, and their role in cholinergic function is supported by their placement and/or proximity to choline acetyltransferase (ChAT), the velocity limiter enzyme that catalyzes ACh synthesis. About 10%-15% cholinergic neurons inside the human hippocampus and amygdala seem to express BuChE rather than aChE. The aChE and BuChE share about 65% amino acid sequence homology although encoded by different genes on human chromosomes 7 (7q22) and 3 (3q26), respectively. However, both bind and split ACh highly and effectively, with slightly different kinetics, making choline and acetic acid metabolic products identical. *The aChE has three residues related to asparagus with carbohydrates and BuChE has nine, which can affect their watery solubility, stability, functional conformation and therefore their biological activity*. In addition, both enzymes can form *disulfide bond with cysteine defined along their sequence* to support their dimerization to generate multiple structural enzymes subunits forms in different brain sites, such as the three globular forms (G forms) that include one (G1), there are mainly two catalytic subunits (G2) or four (G4). *The site associated with ACh hydrolysis is internalized in both enzymes*. The aChE and BuChE both have an active narrow site, mainly hydrophobic, characterized by X-ray crystallography in the order of 20Å depth for aChE, in which ACh spreads and then divides (54). *ACh is involved in inflammatory states modulation*. Recent data shown that ACh, derived from parasympathetic innervations, inhibits *the tumor necrosis factor (TNF-) and interleukin 1 (IL-1) release from macrophages through the nicotinic receptors activation, and the data support an "anticholinergic" inflammatory pathway existence* (46-47-48).

In the central nervous system, nicotinic and muscarinic receptors subtypes are present on both neurons and glial cells where they mediate motor control, memory regulation, temperature regulation (hyperthermia that is difficult to control), synapse and plasticity functions such as auto-heteroreceptors. Within the peripheral nervous system, muscle receptors seem widely involved in several functions, such as smooth muscle contraction, glandular secretion and heart rate regulation (49-50). All cells types within the respiratory tract express muscarinic and nicotinic receptors. Ipratropium and oxitropium (M1/M3 receptors antagonists) and, more recently, tiotropium (non-selective) have an advantage over atropine or other muscarinic antagonists, resulting from their pharmacokinetics; the quaternary ammonium presence in their chemical formula allows a local effect that reduces its absorption by bronchus (51,52,53).

Discussion.

Cholinesterase serves *as possible poisoning indicator mediated by the acetyl cholinesterase enzyme inhibition*. They are used as liver function functionality index. Their blood values are reduced in organophosphorus intoxication, liver dysfunctions (hepatitis, etc.), cirrhosis, myocardial infarction, acute infections and atypical enzyme phenotypes. Atypical forms are traditionally distinguished with the inhibition dibucaine test resistance or fluoride and so with cholinesterase activity (Woman values: normal: > 75%, heterozygous: 50-75%, homozygous: < 50%; Man values: normal: > 75%, heterozygous: 50-75%, homozygous: < 50%). *They are toxins target present in many animal poisons*. Those snake toxins (*Naja Atra* and *Bungarus m. and f.*) are acetylcholinesterase and particular Butyryl cholinesterase (*pseudo cholinesterase*). Some toxins also have similar properties to neuromuscular nicotinic receptor agonists. The toxicity manifests itself in part to an excessive increase in Ach and partly to the nicotinic receptors block: prolonged apnea, cardiocirculatory collapse, heart arrhythmias, ventricular tachycardia, body temperature alteration, electrolyte imbalance (particularly K⁺), butyryl cholinesterase low plasma levels. In the first case the effects are the increase in the Acetylcholine action consequence (M2 receptors: bradycardic effect with slowing heart activity and cardiac range reduction, followed by arrhythmic and tachycardic compensation) and *with other nonspecific neurosensory symptoms*. They result in *generalized vasodilation* resulting in rapid drop in blood pressure; M3 receptors: *huge increase in mucous bronchial*

secretions with vasoconstriction, increased gastrointestinal motility. Local effects are due to aerosol exposure at the contact point through the eyes or respiratory system or followed by local fluid absorption through the skin or mucous, including gastrointestinal tract. The effects duration is largely determined by the toxin characteristics: fat-soluble, whether it should be metabolically activated or not, the toxin-aChE complex stability and the phosphorous enzyme "aging". Eye symptoms include: myosis, eye pain, conjunctive congestion, vision reduction, ciliate spasm and eyebrow pain. As an acute systemic absorption result, myosis is not shown thank to a powerful sympathetic discharge to response hypotension. Other aspects are rhinorrhea and hyperemia; chest constriction sense, breathlessness, bronchus constriction and bronchial secretions increase. Other symptoms will be nausea, vomiting, abdominal cramps and diarrhea. Until we get to the serious effects from high dosage, that are: extreme salivation, involuntary feces and urine emission, sweating, tearing, bradycardia, hypotension, arrhythmias and cardiocirculatory collapse. Nicotinic actions on neuromuscular junctions are muscle fatigue and general weakness, involuntary contractions, spread fasciculations and finally marked weakness increase and respiratory muscles paralysis. The effects on the Snc are confused state, ataxia, verbal confusion, reflexes loss, Cheyne-stokes breath, convulsions, coma and respiratory paralysis. The effects on medulla oblongata vasomotor and other cardiovascular centers lead to hypotension with fibrillation and reflex tachycardia. The muscarinic CNS and nicotinic effects all contribute to respiratory impairment. These included laryngospasm, bronchus-constriction, increased secretions, impaired diaphragm and intercostal muscles movements and respiratory depression. Blood pressure can drop to low levels due to irregularities in heart rhythm, effects caused by hypoxemia and often antagonized by assisted ventilation lung. Nonspecific symptoms can be anosmia and dysgeusia. Olfactory dysfunction is an early Parkinson's disease 'preclinical' sign, often precedes years and remains the only symptom before disease diagnosis that is confirmed when now more than 80% GABAergic neurons are lost. The dysgeusia and anosmia pathophysiological and neuronal mechanism in Parkinson's disease (cholinergic pathways at higher levels) are still being studied. It should be remembered that these neuronal pathways do not pass through the thalamic nucleus but relate directly to the Hippocampus/Amygdala complex.

As Blastn results show besides bungaro-toxins, *phospholipase A2 must be considered*. Phospholipases A2 (PLA2) are among the most abundant proteins in snake venom. They are a 16 groups within six main types superfamily (85,86). They resemble each other for catalytic structures and properties. They have a toxic pharmacological activities broad spectrum as well as being hydrolasis (87). John B. Harris et al. confirm the “PLA2 major types” include the secreted PLA2s (sPLA2), the cytosolic PLA2s (cPLA2), the calcium Independent PLA2s (iPLA2) the platelet activating factor (PAF) acetyl hydrolase/oxidised lipid lipoprotein associated PLA2 (LpPLA2s), the adipose PLA2s (AdPLA2s) and the lysosomal PLA2s (LPLA2s). The hydrolysis of glycerophospholipids by PLA2s results in the fatty acid release and relevant lysophospholipid production (88). Arachidonic acid (AA) is generated by membrane phospholipids through their activation. Prostaglandins are generated in the pathway of cyclooxygenase 1 (COX1). They are generated together the enzyme thromboxane synthetase thromboxane A2(TXA2), a powerful platelet aggregant. COX1 FANS inhibition leads to an increase in the lipoxygenase pathway with an increase in the final leukotrienes products (LB4, LC4, LD4, LE4, LF4). The enzyme thromboxane synthetase blockage, by Dazoxiben and Pirmagrel, leads to an increase in the prostaglandins synthesis through the isomerases (PGD2, PGF2alfa, PGE2) and prostacyclin synthetase (PGI2, PGF1 alpha). PGE is a powerful vasodilator. In all human districts causes both vasodilation and vasoconstriction but in the pulmonary circle only vasoconstriction. The cardiac output increases by PGE and PGF. Thromboxane A2 is vasoconstriction molecule and results in platelet aggregation, decrease the kidney blood flow and its filtration (82). *There is an increase in thromboembolic events. PGF and PGD2 induce the bronchial and tracheal muscles contraction, while PGE relaxation.* Asthmatic and COPD individuals are very sensitive to PGF2. LTC4 and LTD4 are a thousand times more potent than histamine, act on the smooth muscles of the peripheral respiratory tract and are bronchoconstrictor (89-92). PLA2 induces inflammation with mediators’ release including IL-1 β , IL-6, IL-8, TNF- α , MIP-1 α , NO, histamine, serotonin, PAF, bradichinine, PGE2, TXA2, LTB4, RANTES and anaphylatoxins (C3 and C5) (93). *Dexamethasone inhibits the prostaglandins synthesis and leukotriene formation (94), also inhibit them at the cyclooxygenase/PGE isomerase level (95).* It works by inhibiting PLA2, also inhibits cytokines IL1, IL2,

IL3, Il6, TNF-alfa, GM-CSF, interferon range. The dexamethasone inhibits the epidermal growth factor (EGF)-stimulated by PLA2 (cPLA2) and the AA release by blocking the Grb2 recruitment to the activated EGF receptor (EGF-R) through a transcription-independent mechanism (actinomycin-insensitive) (96).

Considerations.

Blastn alignment suggests a good correlation between the Covid-19 and bungaro-toxins genetic sequence, phospholipase A2 and the similar prothrombin activator protein. The snake can be considered as an intermediate natural host (axiom 1,2,3,8,9 respected) and age variables, phenotype, sex, drugs intake, pre-existing pathologies, special work exposures (health workers, pesticide growers, etc.) may be related and dependent to the viral charge concentration, toxins released and both immune system and cholinesterase functionality (axioms 4,5,6,7 respected). It is not so much essential to know the intermediate host as to understand if the virus can express similar properties. The crazy hypothesis, initially defined as "Absurd - reductio ad absurdum", is very likely to be true.

Below is suggested (Figure 6) a new Covid-19 Virus double pathogenic model, evolved. It is a respiratory virus like a "Trojan- horse", which in passing through the intermediate host has probably acquired, randomly and naturally, simple or small gene sequences (micro-rna?). Such sequences may be similar, but also split (gene recombination model in natural way). They will probably be transcribed like the originals by 3D globular profile, with same folds number about, charges, the sulfide bond number, mostly for the key amino acids position along the protein chain. They don't necessarily must have the same amino acid length. They can be shorter provided they adapt with at least two or more faces to the binding site receptors, respecting the loops rules, electrostatic charges and key amino acids who are necessary at binding receptor interface. These molecules synthesis is defined as "factors". We could imagine this mechanism very similar to the atomic orbitals Aufbau principle, with the electron's distribution according to the Hund rule (84). The interaction factors and receptors give strength to the viremia. We call these molecules as "The Zero Point Factors". It generates a circuit (loop): faster the viremia and replication are, more factors/toxins are translated, and more viremia will increase thanks to the latter action on the immune system. On the other hand, the immune system also has significant interindividual variations in age, genetics, pathologies,

etc. *Longer time the immune system takes to produce antibodies against virus, more factors are released in the circulation and more the immune system is blocked by the viremia and factors double synergistic action.* In this model, the decisive conditions are the exposition time, the initial and/or repeated viral load (number viral particles/ Inhaled air volume). More longer exposition, occasional or not, simple or repeated, more higher the started viral load is and more the outcome will be subordinate to the toxic state achieved, to the immune system efficiency, to the efficacy enzymes (aChE and buChE) and the antiviral or support therapies adopted. The virus uses its greed for ACE2 receptors. *Zero-point Factors would act at the central and peripheral cholinergic synapses level, and on nicotinic receptors, on clotting factors by enhancing the the COVID-19 virus pathogenicity.* Subjects would therefore be at greater risk: any with ACE2r over-expression (taking drugs-inib. Ace.); health worker, for the increase in exposition time; a low immune system (oncology, autoimmune diseases, treatment with immunosuppressants, etc.) subjects; heart and respiratory diseases (for both toxicity factors produced and viremia) patients; lower levels or altered cholinesterase functioning (different by age, gender, race and phenotype); neuronal diseases such as Parkinson's (PD), Alzheimer's (AD), etc. or autoimmune such as Myasthenia Gravis patients that being treated with acetylcholinesterase inhibitors; growers with seasonal exposition to organophosphorus (pesticides). A single factor possibility showing dose/dependent receptor affinity first towards the cholinesterase and then, increased doses, dependent viremia, towards the nicotinic receptors with blocking action is not excluded. *The outcome would depend on the dual pathogen action mechanism: on the one hand the viremia elements and on the other the toxicity factors.*

Conclusions.

The actual therapies practiced are: Lopinavir/ Ritonavir, Chloroquine, Remdesivir, Ribavirin Synthetic, Oseltamivir, Penciclovir/Acyclovir, Ganciclovir, Favipiravir (2, 30). The actual therapies in trial are: Darunavir/cobicistat; Lopinavir/ritonavir; Tocilizumab (83).

The Blast results show some factors like protein that can be implicated such as *bungaro-toxins, phospholipase A2 and the similar prothrombin activator protein.*

Toxins are generally weakly immunogenic and therefore often not effectively targeted by current polyclonal antivenom therapies (31). *NACHR*

imitations, also known as acetylcholine binding proteins (AChBPs), can capture toxins and thus be used to prevent neurotoxic envenoming (31). While waiting for a vaccine solution against the surface virus antigens, valid until the virus will change its recognition characteristics, it would be appropriate to evaluate the suggested data and consider *convalescent blood products (CBPs)* since they would act not only against the pathogen Covid-19 but also towards the likely factors produced by it (22). The human cholinesterase derivative huBuChE administration (*im*) (40) could be studied as an adjuvant. The *antibodies monoclonal* use, probably directed either towards the virus surface antigens and/or towards the foreign factors transcribed from it, could be an immediate solution and allow to contain the mortality rates. Some authors studying the Pyridostigmine bromide and huperzine A use against nerve agent poisonings (GD), have implemented a fast protocol for *cholinesterase* dosage, with the full blood test *WRAIR WBAIR*, US patent No. 6,746,850 help (45). Both the latter and the *feature test*, dibucaine inhibition (41-42) could be associated with the nasal and/or oropharynx swab (time and sensitive operator), could be used as a criterion and parameter to define the hospitalization and patients outcome, to stratify the risk and to integrate therapeutic possibilities. PLA2 can be dosed with the Abcam Secretary PLA2 Assay Kit ab133089 or other similar test. Such tests could be a valuable tool for interception, monitoring and clinical evaluation. *The S100 protein could be used to test outcomes patients during the mechanical ventilation* (42). The genesis, "zero point", identification remains a crucial and fundamental moment. The *sylllogism* is simplified in the following scheme: Beta coronaviruses hold "X" with them; some snakes produce "Y*Z"; covid-19 certainly has an "intermediate host" ; Mr. Blast says that covid-19 and snake toxins are "probably related"; The Covid-19 virus is a beta coronavirus and has "X+Y*Z". *The result is final syllogism: the Covid-19 virus can be a beta coronavirus with toxic factors*. It may seem like a basic logic, but the blast data integrated with the observations suggests that conclusion. The autonomic nervous system study is complex and full molecular, sub-molecular, atomic mechanisms, still unknown. Current knowledge is essential to better differentiate and catalogue the symptoms manifestation. Magnificent ancestral system signs and/or symptoms, while going unnoticed, may allow for a reverse deductive and inductive process,

that is, from the end to the likely beginning. Clinical trials, research, patterns analysis acquired by the animal and plant kingdom historical knowledge and how they interact with other living beings can help as well as the medical, mathematical, statistical, epidemiological, physical and chemical branches integration in better understanding our autonomous system and its functions.

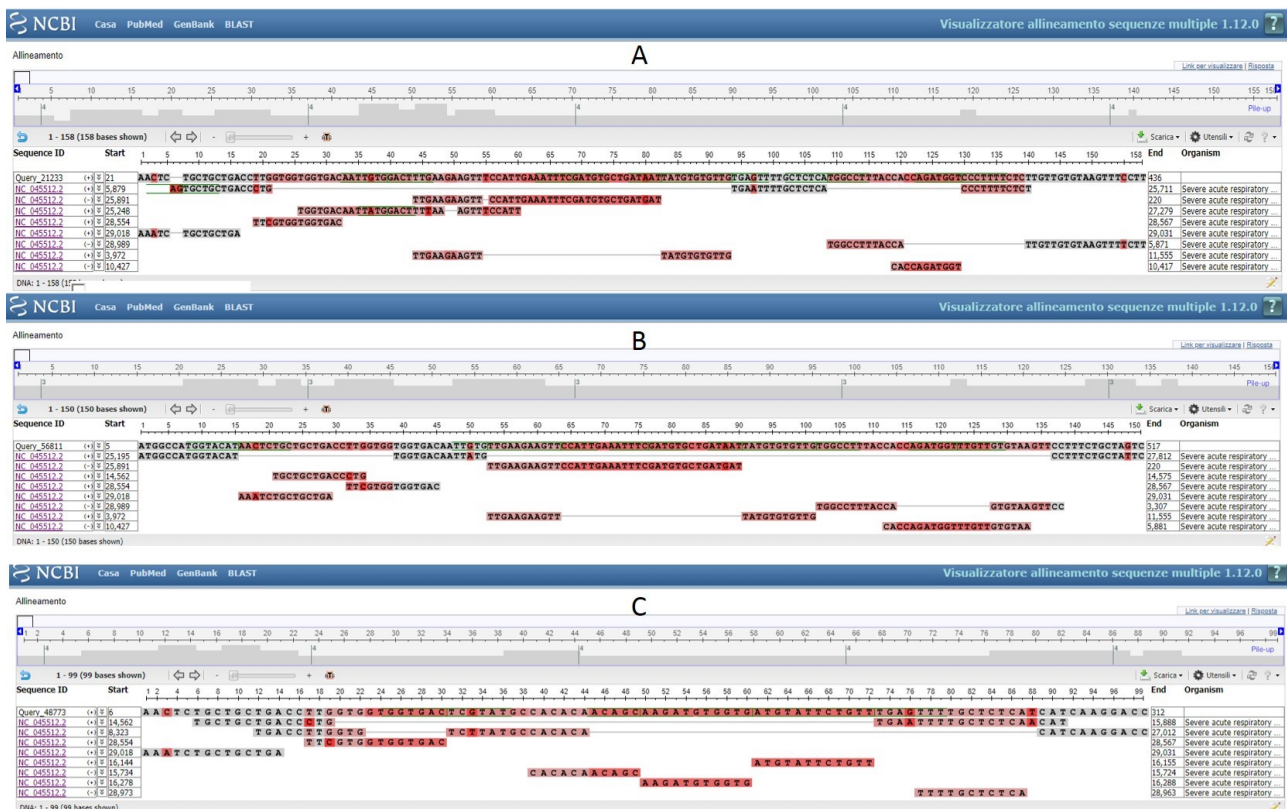


Fig 1 -B. Multicinctus peptide 1 similar to neurotoxin (NL1) (X64593.1), Query cover 32%, e-value 0.5, 100% identity percentage (Figure 1A); Cardiotoxin VII Naja atra (id. U42584.1), Q.C. 26%, e-v. 0.048, for. Id. 100% (fig 1B); Bungarotoxin (V31) Bungarus multicinctus alpha- (id. Y17057.1) Q.C 31%, e-v.0.092 for. Id 89.47% (Fig 1C).

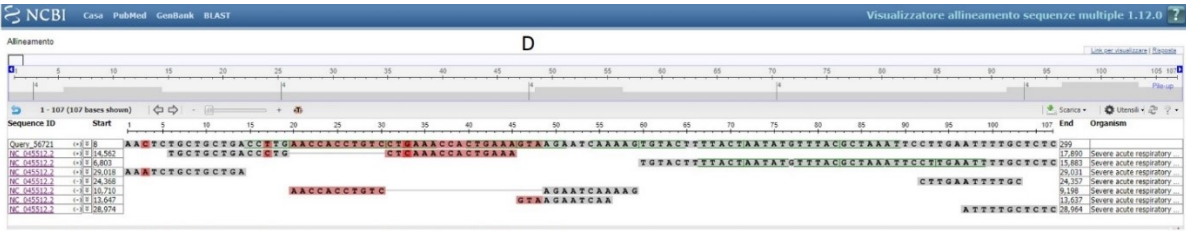


Fig 2.D Clone pGEMT-BMNTL4 Bungarus multicinctus AJ007764.1



fig 2.E -Alpha-bungarus 3ftx Type II CAB51841.1

Fig.2 Bungarus multicinctus mRNA (Clone pGEMT-BMNTL4 id. AJ007764.1) Q.C. 33%, e-v 0.092 for. Id. 100.00% (fig 2.D); Alpha- bungarus3ftx Type II (id. CAB51841.1) Query 32%, e-v. 0.14, per.Id. 93.75% (Figure 2.E).



Fig.3 G-Prothrombin activator Tropidechis ca. DQ533832.1 query 32% ed e-value 0.003

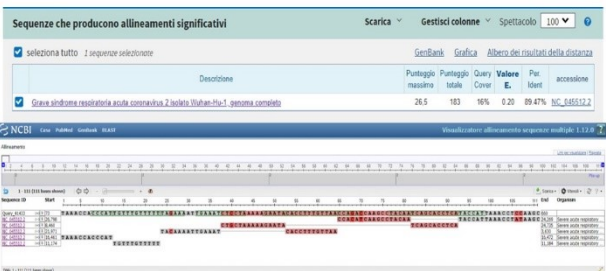
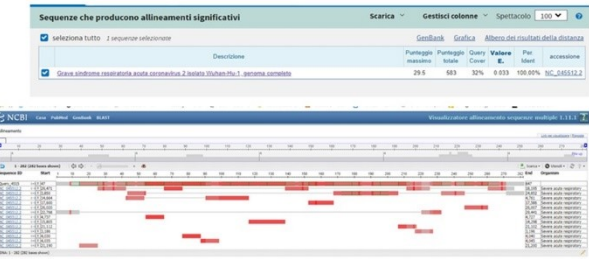


Fig 3. F -Beta bungaratoxin B2a chain Bungarus ca AAL30066.1



pla2 gene for phosph. Laticauda la. AB062441.1

Fig 3 Bungarus ca Beta bungaratoxin B2a chain. (id. AAL30066.1) Q.C. 54%, e-v. 0.19, per.id. 93.33% (fig 3 F); Tropidechis ca. Prothrombin activator (DQ533832.1) Q.C. 32%, e-v. 0.003, per.id. 100% (fig 3.G); Laticauda la PLA2 gene for phosph.. (id. AB062441.1) Q.C. 16%, e-v. 0.2, per.id. 89.47% (fig 3.H).

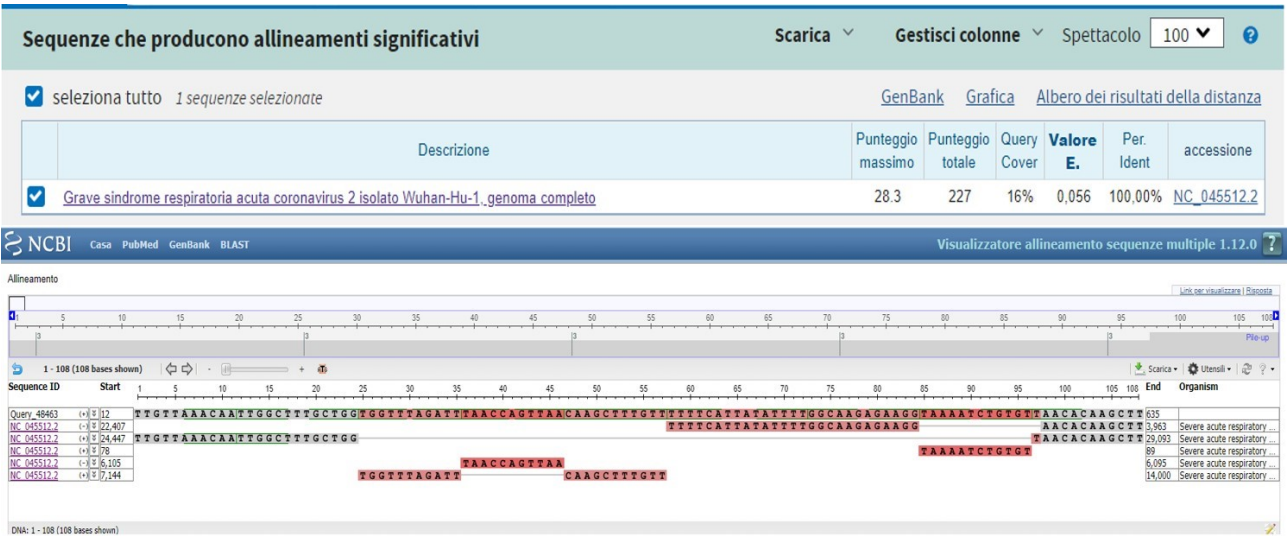
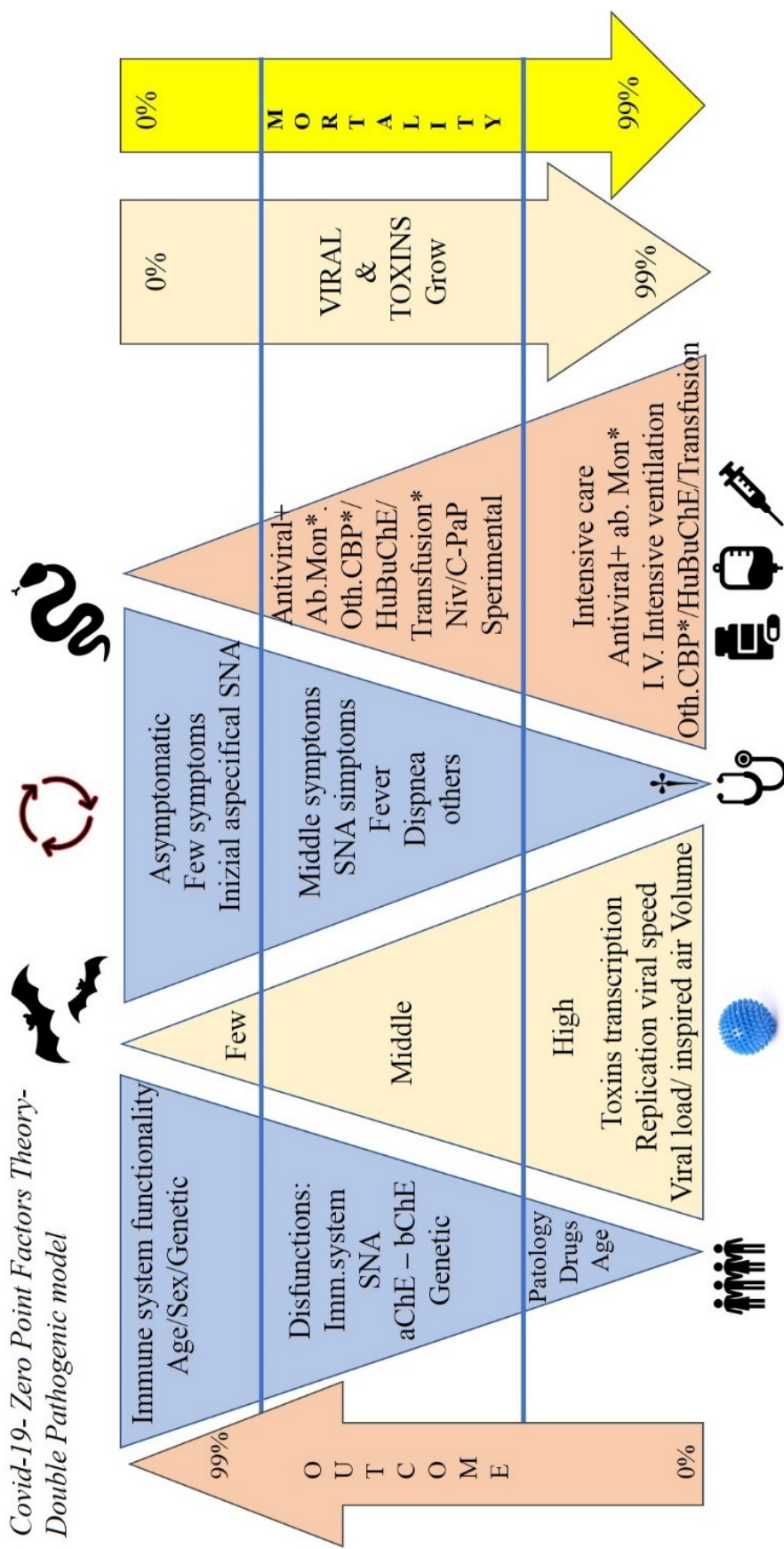


Fig.4 - gene precursor di Ophiophagus hannah Ohanin (king naja), DQ103590.1

Figure 4 Ophiophagus hannah Ohanin (king naja) Gene precursor, (DQ103590.1) Q.C. 16%, e-v.0.056, id.100% (fig 4.).

descrizioni	Riepilogo grafico	allineamenti
Sequenze che producono allineamenti significativi		
Scarica Gestisci colonne Mostrare 100		
seleziona tutto 36 sequenze selezionate		
Descrizione		GenBank Grafica Albero dei risultati della distanza
	Punteggio massimo	Punteggio totale Query Cover Valore E. Per Ident accessione
<input checked="" type="checkbox"/> Manis.pentadactyla Isolare.MPE899 Impalcatura genomica non posizionata Scaffold795 .sequenza del fucile a tutto genoma	50.0	50.0 0% 0.11 86.36% KN006412.1
<input checked="" type="checkbox"/> Manis.pentadactyla Isolare.MPE899_M.pentadactyla:1.1.1-795.6 .sequenza del fucile a tutto genoma	50.0	50.0 0% 0.11 86.36% JPTV01013867.1
<input checked="" type="checkbox"/> Manis.pentadactyla Isolare.MPE899 Impalcatura genomica non posizionata Scaffold4935 .sequenza di fucili a tutto genoma	47.3	47.3 0% 1.4 87.50% KN010531.1
<input checked="" type="checkbox"/> Manis.pentadactyla Isolare.MPE899 Impalcatura genomica non posizionata Scaffold10218 .sequenza del fucile a tutto genoma	47.3	47.3 0% 1.4 86.96% KN015718.1
<input checked="" type="checkbox"/> Manis.pentadactyla Isolare.MPE899_M.pentadactyla:1.1.1-10218.2 .sequenza del fucile a tutto genoma	47.3	47.3 0% 1.4 86.96% JPTV01086931.1
<input checked="" type="checkbox"/> Manis.pentadactyla Isolare.MPE899_M.pentadactyla:1.1.1-4935.1 .sequenza del fucile a tutto genoma	47.3	47.3 0% 1.4 87.50% JPTV01053565.1
<input checked="" type="checkbox"/> Manis.pentadactyla Isolare.MPE899 Impalcatura genomica non posizionata Scaffold2478 .sequenza del fucile a tutto genoma	46.4	46.4 0% 1.4 93.33% KN008090.1
<input checked="" type="checkbox"/> Manis.pentadactyla Isolare.MPE899 Impalcatura genomica non posizionata Scaffold5694 .sequenza del fucile a tutto genoma	46.4	46.4 0% 1.4 76.92% KN011287.1
<input checked="" type="checkbox"/> Manis.pentadactyla Isolare.MPE899 Impalcatura genomica non posizionata Scaffold9057 .sequenza di fucili a tutto genoma	46.4	46.4 0% 1.4 89.19% KN014577.1
<input checked="" type="checkbox"/> Manis.pentadactyla Isolare.MPE899 Impalcatura genomica non posizionata Scaffold10754 .sequenza del fucile a tutto genoma	46.4	46.4 0% 1.4 93.33% KN016238.1
<input checked="" type="checkbox"/> Manis.pentadactyla Isolare.MPE899_M.pentadactyla:1.1.1-10754.2 .sequenza del fucile a tutto genoma	46.4	46.4 0% 1.4 93.33% JPTV01089796.1
...		
<input checked="" type="checkbox"/> Manis.pentadactyla Isolare.MPE899 Impalcatura genomica non posizionata Scaffold10218 .sequenza del fucile a tutto genoma	47.3	47.3 0% 1.4 86.96% KN015718.1
<input checked="" type="checkbox"/> Manis.pentadactyla Isolare.MPE899_M.pentadactyla:1.1.1-10218.2 .sequenza del fucile a tutto genoma	47.3	47.3 0% 1.4 86.96% JPTV01086931.1
<input checked="" type="checkbox"/> Manis.pentadactyla Isolare.MPE899_M.pentadactyla:1.1.1-4935.1 .sequenza del fucile a tutto genoma	47.3	47.3 0% 1.4 87.50% JPTV01053565.1
<input checked="" type="checkbox"/> Manis.pentadactyla Isolare.MPE899 Impalcatura genomica non posizionata Scaffold2478 .sequenza del fucile a tutto genoma	46.4	46.4 0% 1.4 93.33% KN008090.1
<input checked="" type="checkbox"/> Manis.pentadactyla Isolare.MPE899 Impalcatura genomica non posizionata Scaffold5694 .sequenza del fucile a tutto genoma	46.4	46.4 0% 1.4 76.92% KN011287.1
<input checked="" type="checkbox"/> Manis.pentadactyla Isolare.MPE899 Impalcatura genomica non posizionata Scaffold9057 .sequenza di fucili a tutto genoma	46.4	46.4 0% 1.4 89.19% KN014577.1
<input checked="" type="checkbox"/> Manis.pentadactyla Isolare.MPE899 Impalcatura genomica non posizionata Scaffold10754 .sequenza del fucile a tutto genoma	46.4	46.4 0% 1.4 93.33% KN016238.1
<input checked="" type="checkbox"/> Manis.pentadactyla Isolare.MPE899_M.pentadactyla:1.1.1-10754.2 .sequenza del fucile a tutto genoma	46.4	46.4 0% 1.4 93.33% JPTV01089796.1
<input checked="" type="checkbox"/> Manis.pentadactyla Isolare.MPE899_M.pentadactyla:1.1.1-9057.3 .sequenza del fucile a tutto genoma	46.4	46.4 0% 1.4 89.19% JPTV01080191.1
<input checked="" type="checkbox"/> Manis.pentadactyla Isolare.MPE899_M.pentadactyla:1.1.1-5694.3 .sequenza del fucile a tutto genoma	46.4	46.4 0% 1.4 76.92% JPTV01059006.1
<input checked="" type="checkbox"/> Manis.pentadactyla Isolare.MPE899_M.pentadactyla:1.1.1-2478.5 .sequenza del fucile a tutto genoma	46.4	46.4 0% 1.4 93.33% JPTV01032659.1
<input checked="" type="checkbox"/> Manis.pentadactyla Isolare.MPE899 Impalcatura genomica non posizionata Scaffold11748 .sequenza del fucile a tutto genoma	45.5	45.5 0% 4.7 96.30% KN007363.1
<input checked="" type="checkbox"/> Manis.pentadactyla Isolare.MPE899 Impalcatura genomica non posizionata Scaffold2489 .sequenza del fucile a tutto genoma	45.5	45.5 0% 4.7 96.30% KN008101.1
<input checked="" type="checkbox"/> Manis.pentadactyla Isolare.MPE899 Impalcatura genomica non posizionata Scaffold11289 .sequenza del fucile a tutto genoma	45.5	45.5 0% 4.7 90.62% KN016749.1
<input checked="" type="checkbox"/> Manis.pentadactyla Isolare.MPE899_M.pentadactyla:1.1.1-11289.2 .sequenza del fucile a tutto genoma	45.5	45.5 0% 4.7 90.62% JPTV01092685.1
<input checked="" type="checkbox"/> Manis.pentadactyla Isolare.MPE899_M.pentadactyla:1.1.1-2489.1 .sequenza del fucile a tutto genoma	45.5	45.5 0% 4.7 96.30% JPTV01032797.1
<input checked="" type="checkbox"/> Manis.pentadactyla Isolare.MPE899_M.pentadactyla:1.1.1-1748.5 .sequenza del fucile a tutto genoma	45.5	45.5 0% 4.7 96.30% JPTV01025238.1
<input checked="" type="checkbox"/> Manis.pentadactyla Isolare.MPE899 Impalcatura genomica non posizionata Scaffold1119 .sequenza del fucile a tutto genoma	44.6	44.6 0% 4.7 85.11% KN005736.1
<input checked="" type="checkbox"/> Manis.pentadactyla Isolare.MPE899 Impalcatura genomica non posizionata Scaffold380 .sequenza del fucile a tutto genoma	44.6	44.6 0% 4.7 93.10% KN005997.1
<input checked="" type="checkbox"/> Manis.pentadactyla Isolare.MPE899 Impalcatura genomica non posizionata Scaffold2373 .sequenza di fucili a tutto genoma	44.6	44.6 0% 4.7 73.97% KN007987.1
<input checked="" type="checkbox"/> Manis.pentadactyla Isolare.MPE899 Impalcatura genomica non posizionata Scaffold2861 .sequenza del fucile a tutto genoma	44.6	44.6 0% 4.7 84.62% KN008471.1
<input checked="" type="checkbox"/> Manis.pentadactyla Isolare.MPE899 Impalcatura genomica non posizionata Scaffold45223 .sequenza del fucile a tutto genoma	44.6	44.6 0% 4.7 93.10% KN010818.1
<input checked="" type="checkbox"/> Manis.pentadactyla Isolare.MPE899 Impalcatura genomica non posizionata Scaffold7919 .sequenza del fucile a tutto genoma	44.6	44.6 0% 4.7 93.10% KN013461.1
<input checked="" type="checkbox"/> Manis.pentadactyla Isolare.MPE899 Impalcatura genomica non posizionata Scaffold9068 .sequenza del fucile a tutto genoma	44.6	44.6 0% 4.7 100.00% KN014588.1
<input checked="" type="checkbox"/> Manis.pentadactyla Isolare.MPE899 Impalcatura genomica non posizionata Scaffold9225 .sequenza di fucili a tutto genoma	44.6	44.6 0% 4.7 100.00% KN014742.1
<input checked="" type="checkbox"/> Manis.pentadactyla Isolare.MPE899_M.pentadactyla:1.1.1-9225.2 .sequenza del fucile a tutto genoma	44.6	44.6 0% 4.7 100.00% JPTV01081229.1
<input checked="" type="checkbox"/> Manis.pentadactyla Isolare.MPE899_M.pentadactyla:1.1.1-9068.2 .sequenza del fucile a tutto genoma	44.6	44.6 0% 4.7 100.00% JPTV01080250.1
<input checked="" type="checkbox"/> Manis.pentadactyla Isolare.MPE899_M.pentadactyla:1.1.1-7919.6 .sequenza del fucile a tutto genoma	44.6	44.6 0% 4.7 93.10% JPTV01073573.1
<input checked="" type="checkbox"/> Manis.pentadactyla Isolare.MPE899_M.pentadactyla:1.1.1-5223.3 .sequenza del fucile a tutto genoma	44.6	44.6 0% 4.7 93.10% JPTV01055569.1
<input checked="" type="checkbox"/> Manis.pentadactyla Isolare.MPE899_M.pentadactyla:1.1.1-2861.4 .sequenza del fucile a tutto genoma	44.6	44.6 0% 4.7 84.62% JPTV01036206.1
<input checked="" type="checkbox"/> Manis.pentadactyla Isolare.MPE899_M.pentadactyla:1.1.1-2373.6 .sequenza del fucile a tutto genoma	44.6	44.6 0% 4.7 73.97% JPTV01031651.1
<input checked="" type="checkbox"/> Manis.pentadactyla Isolare.MPE899_M.pentadactyla:1.1.1-380.3 .sequenza del fucile a tutto genoma	44.6	44.6 0% 4.7 93.10% JPTV01007818.1
<input checked="" type="checkbox"/> Manis.pentadactyla Isolare.MPE899_M.pentadactyla:1.1.1-119.15 .sequenza del fucile a tutto genoma	44.6	44.6 0% 4.7 85.11% JPTV01002942.1

Fig 5 (“Manis pentadactyla”).



* probable the quickest and cheapest solution- Dr. Carlo Brogna-Italy

Fig 6- New probable double pathogenic model (M.D.Carlo Brogna)

References:

1. Arinjay Banerjee, et All in *Viruses* 2019,11,41;(doi: 10.3390/v11010041) “Bats and Coronaviruses”;
2. Yan-Rong Guo^{1†} et All (The origin, transmission and clinical therapies on coronavirus disease 2019 (COVID-19) outbreak – an update on the status- A novel coronavirus from patients with pneumonia in China, 2019. *N Engl J Med.* 2020;382(8): 727–33);
3. Giovanetti M, Benvenuto D, Angeletti S, Ciccozzi M. The first two cases of 2019-nCoV in Italy: where they come from? *J Med Virol.* 2020:1–4. Paraskevis D, Kostaki EG, Magiorkinis G, Panayiotakopoulos G, Sourvinos G, Tsiodras S. Full-genome evolutionary analysis of the novel corona virus (2019-nCoV) rejects the hypothesis of emergence as a result of a recent recombination event. *Infect Genet Evol.* 2020; 79:104212;
4. Zhou P et All (A pneumonia outbreak associated with a new coronavirus of probable bat origin. *Nature* 2020;
5. Liu Z, Xiao X, Wei X, Li J, Yang J, Tan H, et al. Composition and divergence of coronavirus spike proteins and host ACE2 receptors predict potential intermediate hosts of SARS-CoV-2. *J Med Virol.* 2020;
6. Wu F, Zhao S, Yu B, Chen YM, Wang W, Song ZG, et al. A new coronavirus associated with human respiratory disease in China. *Nature.* 2020;
7. de Wit E, van Doremalen N, Falzarano D, Munster VJ. SARS and MERS: recent insights into emerging coronaviruses. *Nat Rev Microbiol.* 2016;14(8):523–34;
8. Song Z, Xu Y, Bao L, Zhang L, Yu P, Qu Y, et al. From SARS to MERS, thrusting coronaviruses into the spotlight. *Viruses*. 2019;11(1): E59. <https://doi.org/10.3390/v11010059> e Cui J, Li F, Shi ZL. Origin and evolution of pathogenic coronaviruses. *Nat Rev Microbiol.* 2019;17(3):181–92;
9. Angeletti S, Benvenuto D, Bianchi M, Giovanetti M, Pascarella S, Ciccozzi M. COVID-2019: the role of the nsp2 and nsp3 in its pathogenesis. *J Med Virol.*2020;
10. Zhang L, Shen FM, Chen F, Lin Z. Origin and evolution of the 2019 novel coronavirus. *Clin Infect Dis.* 2020. <https://doi.org/10.1093/cid/ciaa112> [Epub ahead of print];
11. Jia HP, Look DC, Shi L, Hickey M, Pewe L, Netland J, et al. ACE2 receptor expression and severe acute respiratory syndrome coronavirus infection depend on differentiation of human airway epithelia. *J Virol.* 2005;79(23): 14614–21;
12. Wan Y, Shang J, Graham R, Baric RS, Li F. Receptor recognition by novel coronavirus from Wuhan: an analysis based on decade-long structural studies of SARS. *J Virol.* 2020;
13. Tortorici MA, et. Al 2019 Veelsler D. Structural insights into coronavirus entry. *Adv Virus Res.* 2019; 105:93–116;
14. Sawicki SG, Sawicki DL. Coronavirus transcription: a perspective. *Curr Top Microbiol Immunol.* 2005; 287:31–55;
15. Hussain S, Pan J, Chen Y, Yang Y, Xu J, Peng Y, et al. Identification of novel subgenomic RNAs and noncanonical transcription initiation signals of severe acute respiratory syndrome coronavirus. *J Virol.* 005;79(9):5288–95. 36;
16. Perrier A, Bonnin A, Desmarests L, Danneels A, Goffard A, Rouille Y, et al. The C-terminal domain of the MERS coronavirus M protein contains a trans-Golgi network localization signal. *J Biol Chem.* 2019;294(39):14406–21;
17. Chen C, Zhang XR, Ju ZY, He WF. Advances in the research of cytokine storm mechanism induced by Corona Virus Disease 2019 and the corresponding immunotherapies. *Zhonghua Shaoshang Zazhi.* 2020;36(0): E005;
18. Liu Y, Zhang C, Huang F, Yang Y, Wang F, Yuan J, et al. 2019-novel coronavirus (2019-nCoV) infections trigger an exaggerated cytokine response aggravating lung injury. 2020;
19. Liu Q, Wang R, Qu G, Wang Y, Liu P, Zhu Y, et al. General anatomy report of novel coronavirus pneumonia death corpse. *J Forensic Med.* 2020;36(1):19–21.)
20. Kawai T, Akira S. The role of pattern-recognition receptors in innate immunity: update on toll-like receptors. *Nat Immunol.* 2010;11(5):373–84;
21. Wei Ji et al. 2020 | Wei Wang | Xiaofang Zhao | Junjie Zai | Xingguang Li (Cross-species transmission of the newly identified coronavirus 2019-nCoV) *J Med Virol.* 2020; 92:433–440;
22. Convalescent plasma: new evidence for an old therapeutic tool? Giuseppe Marano¹, Stefania Vaglio^{1,2}, Simonetta Pupella¹, Giuseppina Facco^{1,3}, Liviana Catalano¹, Giancarlo M. Liumbruno¹, Giuliano Grazzini¹ *Blood Transfus* 2016; 14: 152-7 DOI 10.2450/2015.0131-15;
23. Dawei Wang , Bo Hu 1, Chang Hu , Fangfang Zhu , Xing Liu , Jing Zhang , Binbin Wang , Hui Xiang , Zhenshun Cheng , Yong Xiong , Yan Zhao , Yirong Li , Xinghuan Wang , Zhiyong Peng Affiliations expand PMID: 32031570 PMCID: PMC7042881 (available on 2020-08-07) DOI: 10.1001/jama.2020.1585 JAMA 2020 Feb 7[Online ahead of print Clinical Characteristics of 138 Hospitalized Patients With 2019 Novel Coronavirus-Infected Pneumonia in Wuhan, China;
24. Huang, Yeming Wang, Xingwang Li, Lili Ren, Jianping Zhao, Yi Hu, Li Zhang, Guohui Fan, Jiuyang Xu, Xiaoying Gu, Zhenshun Cheng, Ting Yu, Jiaan Xia, Yuan Wei, Wenjuan Wu, Xuelei Xie, Wen Yin, Hui Li, Min Liu, Yan Xiao, Hong Gao, Li Guo, Jungang Xie, Guangfa Wang, Rongmeng Jiang, Zhancheng Gao, Qi Jin, Jianwei Wang[†], Bin Cao[†] Clinical features of patients infected with 2019 novel coronavirus in Wuhan, China *Chaolin Lancet* 2020; 395: 497–50;

25. ‘Yan-Rong Guo†, Qing-Dong Cao†, Zhong-Si Hong†, Yuan-Yang Tan, Shou-Deng Chen, Hong-Jun Jin, Kai-Sen Tan, De-Yun Wang and Yan Yan) *Mil Med Res.* 2020; 7: 11 The origin, transmission and clinical therapies on coronavirus disease 2019 (COVID-19) outbreak – an update on the status;
26. Burnouf T, Seghatchian J *Transfus Apher Sci.* Ottobre 2014; 51 (2): 120-5. Ebola Virus Convalescent Blood Products: Where We Are Now and Where We May Need to Go;
27. Vulfius et al (, *PLOS ONE* | DOI: 10.1371/journal.pone.0115428 December 18, 2014;
28. Denis Servent†§, Valérie Winckler-Dietrich†, Hai-Yan Hu, Pascal Kessler†, Pascal Drevet†, Daniel Bertrand and André Ménez†. Only Snake Curare-mimetic Toxins with a Fifth Disulfide Bond Have High Affinity for the Neuronal $\alpha 7$ Nicotinic Receptor* (*J. Biol. Chem.* 272, 24279–24286;
29. Chiappinelli R. e all. (Dipartimento di Farmacologia, Harvard Medical School, Boston, Massachusetts 02115 Comunicato da Stephen W. Kuffler, il 21 marzo 1978;
30. Liying Dong, Shasha Hu, Jianjun Gao Discovering drugs to treat coronavirus disease 2019 (COVID-19) *Drug Discoveries & Therapeutics.* 2020; 14(1):58-60;
31. Laura-Oana Albulescu et al *Front Pharmacol.* 30 lug 2019; 10: 848. doi: 10.3389 -A Decoy-Receptor Approach Using Nicotinic Acetylcholine Receptor Mimics Reveals Their Potential as Novel Therapeutics Against Neurotoxic Snakebite;
32. Di Shoen-Yn shiau lin, chin liao e c. Y. Lee (*Biochimica. J.* (1977) 161.229-232 Mechanism of cardiotoxin, Protaxin and Polyislin anticholinesterase activities);
33. Selvanayagam Nirthanan e Matthew C.E. Gweel (Three fingers -Neurotoxins and the nicotinic acetylcholine receptor, Forty years later *Pharmacol Sci* 94, 1 – 17 (2004);
34. Da c. y. lee, c. c. Chang e k. kamijo 1955 (The Pharmacological Institute, College of Medicine, National Taiwan University, Taipei, Formosa, China, and the Department of Physiology and Pharmacology, Graduate School of Medicine, University of Pennsylvania, Philadelphia, Pennsylvania, United States -Received July 23, 1955) Cholinesterase Inattivazione di Snake Venoms;
35. Edward Chia-Cheng Lai, et al (Comparative risk of pneumonia among new users of Cholinesterase Dementia Inhibitors *J Am Geriatr Soc.* 2015 maggio; 63(5): 869–876. doi: 10.1111/jgs.13380);
36. Catherine A. et al (Inhibition of nicotinic acetylcholine receptors, a new facet in the Pleiotropic Activity of Snake Venom Phospholipases A2 *PLOS ONE* | DOI: 10.1371/ journal. pone.0115428 December 18, 2014);
37. Vivitri Prasasty, Muhammad Radifar ed Enade Istyastono (Natural peptides in targeting for the discovery of Acetylcholinesterase drugs- *Molecules* 2018, 23, 2344; doi: 10.3390/molecules23092344 www.mdpi.com/journal/molecules);
38. Masahiro Seo et al, (Prognostic Significance of Serum Cholinesterase Level in Patients With Reduced, Mid-Range and Preserved Left Ventricular Ejection Fraction With Acute Decompensated Heart Failure: A Prospective Study in Osaka Prefectural Acute Heart Failure Registry (OPAR) *Circulation.* 2018;138: A12826;
39. AA.VV (Influence of age, sex and oral contraceptives on the activity of cholinesterase in human blood *Clinical Chemistry* , Volume 21, Issue 10, 1 settembre 1975, Pagine 1393–1395);
40. Mumford H (Human Plasma-Derived BuChE as a Stoichiometric Bioscavenger for Treatment of Nerve Agent Poisoning *Chem Biol Interact* , 203 (1), 160-6 2013 Mar 25;
41. P. DE LONLAY (Ottobre 2006 ORPHA:132) ultima revisione: Butyrylcholinesterase deficiency - Orphanet www.orpha.net/consor/cgi-bin;
42. T. Yardan, et al (The Role of Serum Cholinesterase Activity and S100B Protein in the Evaluation of Organophosphate Poisoning) *Hum Exp Toxicol*, 32 (10), 1081-8 Ottobre 2013;
43. Chen et al 2008 (Prognostic value of sieroic cholinesterase silky activities in patients poisoned by organophosphati *j. ajem.* 2008.07.006);
44. Shenhar et al. (Cholinesterase as biomarkers for parasympathetic dysfunction and inflammation-related disease *J Mol Neurosci*, 53 (3), 298-305 Lug 2014);
45. Gordon Richard K Gordon, Julian R Haigh, Gregory E Garcia, Shawn R Feaster, Michael A Riel, David E Lenz, Paul S Aisen, Bhupendra P Doctor Affiliations expand et al (Oral administration of pyridostigmine bromide and Huperzine A protects whole human blood cholinesterases from ex Vivo exposure to Soman *Chem Biol Interact*, 157-158, 239-46 15 dicembre 2005);
46. Nigel H. Greig, Marcella Reale, e Ada Maria Tata (New advances in pharmacological approaches to the cholinergic system: a overview of the muscarinic receptor ligands and the Cholinesterase *Recente Pat CNS Drug Discov.* 2013 ago; 8 (2): 123–141);
47. (Wessler I, Kilbinger H, Bittinger F, Unger R, Kirkpatrick CJ. The biological role of non-neuronal acetylcholine in plants and humans. *Giapponese J Pharmacol.* 2001; 85: 2–10.;
48. (Rosas-Ballina M, Tracey KJ. Immune system neurology: Neural reflexes regulate immunity. *Neurone.* 2009; 64: 28–32.);
49. Ragheb F, Molina-Holgado E, Cui QL, et al. Pharmacological and functional characterization of muscarinic receptor subtypes in the development of oligodendrocytes. *J Neurochem.* 2001; 77: 1396–1406;

50. De Angelis F, Bernardo A, Magnaghi V, Minghetti L, Tata AM. Subtypes of muscarinic receptors as potential targets to modulate the survival, proliferation and differentiation of the progenitors of oligodendrocytes. *Dev. Neurobiol.* 2012; 72: 713–728;
51. Oki T, Maruyama S, Takagi Y, Yamamura HI, Yamada S. Characterization of muscarinic receptor binding and inhibition of salivation after oral administration of tolterodine in mice. *Europ J Pharmacol.* 2006; 529:157–163;
52. Racke K, Jurgens UR, Matthiesen S. Control by cholinergic mechanisms. *Eur J Pharmacol.* 2006; 533:57–68.; Racke K, Matthiesen S. The airway cholinergic system: physiology and pharmacology. *Pulm Pharmacol Ther.* 2004; 17:181–198.;
53. Keam SJ, Keating GM. Tiotropium bromide. A review of its use as maintenance therapy in patients with COPD. *Treat Resp Med.* 2004; 3:247–268;
54. Darvesh S, Hopkins D, Geula C. Neurobiology of butyrylcholinesterase. *Nat Rev Neurosci.* 2003; 4:131–138. Darvesh S, Cash MK, Reid GA, Martin E, Mitnitski A, Geula C. Butyrylcholinesterase in associated with β -amyloid plaques in the transgenic APPSW/PSEN1dE9 mouse model of Alzheimer disease. *J Neuropathol Exp Neurol.* 2012 Jan; 71:2–14. Darvesh S, Grantham DL, Hopkins DA. Distribution of butyrylcholinesterase in human amygdala and hippocampal formation. *J Comp Neurol.* 1998; 393:374–390 Darvesh S, Reid GA, Martin E. Biochemical and histochemical comparison of cholinesterases in normal and Alzheimer brain tissues. *Curr Alzheimer Res.* 2010; 7:386–400;
55. Soreq H, Zakut H. Human Cholinesterases and Anticholinesterases. New York: Academic Press; 1993.; Soreq H, Seidman S. Acetylcholinesterase - New roles for an old actor. *Nat Rev Neurosci.* 2001; 2:294–302.;
56. Perry EK, Perry RH, Blessed G, Tomlinson BE. Changes in brain cholinesterase in senile dementia of Alzheimer's type. *Neuropathol Applied Neurobiol.* 1978; 4:273–277;
57. Wright CI, Geula C, Mesulam MM. Neurological cholinesterases in the normal brain and in Alzheimer's disease: relationship to plaques, tangles, and patterns of selective vulnerability. *Ann Neurol.* 1993; 34:373–384.;
58. Eng LF, Uyeda CT, Chao LP, Wolfgram F. Antibody to bovine choline acetyltransferase and immunofluorescent localisation of the enzyme in neurons. *Nature.* 1974; 250:243–245;
59. Greig NH, Sambamurti K, Yu QS, Perry T, Holloway HW, Haberman F, et al. In: Butyrylcholinesterase its Function and Inhibitors. Giacobini E, editor. London: Martin Dunitz; 2003.pp. 69–90;
60. Greig N, Utsuki T, Yu Q, Zhu X, Holloway HW, Perry T, et al. A new therapeutic target in AD treatment: Attention to butyrylcholinesterase: *Cur Med. Res Opinions.* 2001; 17:1–7;
61. Greig NH, Lahiri DK, Sambamurti K. Butyrylcholinesterase: an important new target in Alzheimer's disease therapy. *International Psychogeriatrics.* 2002; 14:77–91;
62. Masson P, Carletti E, Nachon F. Structure, activities and biomedical applications of human butyrylcholinesterase. *Protein Pept Lett.* 2009; 16:1215–1224 151;
63. Silman I, Sussman JL. Acetylcholinesterase: how is structure related to function? *Chem Biol Interact.* 2008; 175:3–10;
64. Sussman JL, Harel M, Frolow F, Oefner C, Goldman A, Toker L, Silman I. Atomic structure of acetylcholinesterase from *Torpedo californica*: a prototypic acetylcholine-binding protein. *Science.* 1991; 253:872–879);
65. Antil-Delbecke I, C Gaillard, T Tamiya, P J Corringer, J P Changeux, D Servent, A Ménez Affiliations expand PMID: 10852927 DOI: 10.1074/jbc.M909746199 *J Biol Chem* 275, 29594-601 2000 Sep 22 Molecular Determinants by Which a Long Chain Toxin From Snake Venom Interacts With the Neuronal Alpha 7-nicotinic Acetylcholine Recepto S;
66. Antil, S., Servent, D. e Ménez, A. (1999) *J. Biol. Chem.* 274, 34851-34858);
67. Ackermann, EJ, Ang, ETH, Kanter, JR, Tsigelny, I. e Taylor, P. (1998) *J. Biol Chem.* 273, 10958-10964);
68. Osaka, H., Malany, S., Molles, BE, Sine, SM, e Taylor, P. (2000) *J. Biol. Chem.* 275, 5478-5484;
69. D Servente, G Mourier, S Antil, A Ménez SMED Expansion Affiliates: 10022254 DOI: 10.1016 / s0378-4274 (98) 00307-5 *Toxicol Lett*, 102-103, 199-203 28 December 1998 How some toxins curaremimetic snakes discriminate against nicotinic acetylcholine receptor subtypes;
70. André Ménez (dal libro La struttura delle tossine degli animali velenosi) *LE SCIENZE* n. 305, gennaio 1994;
71. STOCKER K. (a cura), *Serpents, venins, envenimations*, Société Herpétologique de France, Edition Fondation Marcel Mérieux, 1987.;
72. *Medical Use of Snake Venom Proteins*, CRC Press, Boca Raton, 1990;
73. Harvey, Pergamon Press, 1991 *Snake Toxins*, *International Encyclopedia of Pharmacology and Therapeutics*, a cura di A. H.;
74. MENEZ A. e altri, in «Proceedings of the Royal Society of Edinburgh», 99B, pp. 83-102, 1992.;
75. BONTEMS F. e altri, in «Science», n. 254, pp. 1521-1523.;
76. R Manjunatha Kini nel “Molecular moulds with multiple missions: functional sites in three-finger toxins *Clinical and Experimental Pharmacology and Physiology* (2002) 29, 815–822;
77. Aisha Munawar, Syed Abid Ali, Ahmed Akrem and Christian Betzel presentano una review dal titolo “Snake Venom Peptides: Tools of Biodiscovery” *Toxins* 2018, 10, 474; doi:10.3390/toxins10110474;

78. Harald k.l.et all. Van den born,'3 zoran radic,'* pascale marchot,'v4 palmer taylor,' and igor tsigelny's2 "Theoretical analysis of the structure of the peptide fasciculin and its docking to acetylcholinesterase". Protein Science (1995), 4:703-715. Cambridge University Press. Printed in the USA.;
79. Venaa RAO*, Jeremiah S. JOSEPH† and R. Manjunatha KINI*‡Biochem. J. (2003) 369, 635–642 (Printed in Great Britain) 635 Group D prothrombin activators from snake venom are structural homologues of mammalian blood coagulation factor Xa Veena S1;
80. M. Chatterjee ; M. Manke ; M. Cebo ; J. Rheinlaender ; A. Witte ; T. Schäffer ; M. Lämmerhofer ; O. Borst ; M. Gawaz CXCR7 chemokine platelet receptor Media an antithrombotic and antithrombamine effectCXCR7 chemokine platelet receptor Media an antithrombotic and antithrombamine effectRes Pract Thromb Haemost . Luglio 2018; 2 (Suppl 1): 1–368.Pubblicato online il 5 luglio 2018: 10.1002 / rth2.12125;
81. E.K. Perry, R.H. Perry, C.J. Smith, D. Purohit, J. Bonham, D.J. Dick, J.M. Candy, Cholinergic Receptors in Cognitive Disorders J. A. Edwardson and A. Fairbairn Can. J. Neurol. Sci. 1986; 13:521;
82. Manual Goodman & Gilman. The pharmacological basis of drug therapy Laurence L. Brunton, Randa Hilal-Dandan, e al. |2018;
83. Note AIFA Italia dal 11 Marzo in poi https://www.aifa.gov.it/documents/20142/1131319/covid-19_sperimentazioni_in_corso_27.03.2020.pdf/b2391bac-7920-0945-51a1-66db453053cf.
84. IUPAC. A compendium of chemical terminology, 2nd ed. (the "Golden Book"). Compiled by AD McNaught and A. Wilkinson. Blackwell Scientific Publications, Oxford (1997). Online version (2019-) created by SJ Chalk. ISBN 0-9678550-9-8. <https://doi.org/10.1351/goldbook>
85. Burke, J.E.; Dennis, E.A. Phospholipase A2 structure/function, mechanism and signaling. J. Lipid Res. 2008, 50, S237–S242.
86. Dennis, E.A.; Cao, J.; Hsu, Y.-H.; Magrioti, V.; Kokotos, G. Phospholipase A2 enzymes: Physical structure, biological function, disease implication, chemical inhibition and therapeutic
87. Raoudha Zouari-Kessentini, Najet Srhiri-Abid, Amine Bazaa, Mohamed El Ayeb, Jose Luis, and Naziha Marrakchi. Antitumoral Potential of Tunisian Snake Venoms Secreted Phospholipases A2 Biomed Res Int. 2013; 2013: 391389. Published online 2013 Jan 31. doi: 10.1155/2013/391389 PMID: 23509718
88. John B. Harris†, and Tracey Scott-Davey Secreted Phospholipases A2 of Snake Venoms: Effects on the Peripheral neuromuscular System with Comments on the Role of Phospholipases A2 in Disorders of the CNS and Their Uses in Industry Toxins (Basel). 2013 Dec; 5(12): 2533–2571. Published online 2013 Dec 17. doi: 10.3390/toxins5122533 PMID: PMC3873700 PMID: 24351716
89. E. A. Dennis, "Phospholipase A2 in eicosanoid generation," *American Journal of Respiratory and Critical Care Medicine*, vol. 161, no. 2, part 2, pp. S32–S35, 2000.
90. T. J. Shuttleworth, "Arachidonic acid activates the noncapacitative entry of Ca²⁺ during [Ca²⁺] *i* oscillations," *Journal of Biological Chemistry*, vol. 271, no. 36, pp. 21720–21725, 1996.
91. M. N. Graber, A. Alfonso, and D. L. Gill, "Ca²⁺ pools and cell growth: arachidonic acid induces recovery of cells growth arrested by Ca²⁺ pool depletion," *Journal of Biological Chemistry*, vol. 271, no. 2, pp. 883–888, 1996.
92. C. D. Funk, "Prostaglandins and leukotrienes: advances in eicosanoid biology," *Science*, vol. 294, no. 5548, pp. 1871–1875, 2001
93. Catarina Teixeira, Cristina Maria Fernandes, Elbio Leiguez, and Ana Marisa Chudzinski-Tavassi, Inflammation Induced by Platelet-Activating Viperid Snake Venoms: Perspectives on Thromboinflammation Immunol. 2019; 10: 2082. Published online 2019 Sep 4. doi: 10.3389/fimmu.2019.02082 PMID: PMC6737392 PMID: 31572356
94. M. Goppelt-Strube, D. Wolter, and K. Resch Glucocorticoids inhibit prostaglandin synthesis not only at the level of phospholipase A2 but also at the level of cyclo-oxygenase/PGE isomerase. Br J Pharmacol. 1989 Dec; 98(4): 1287–1295. doi: 10.1111/j.1476-5381.1989.tb12676.x PMID: PMC1854794 PMID: 2514948
95. M. Goppelt-Strube, D. Wolter, and K. Resch Glucocorticoids inhibit prostaglandin synthesis not only at the level of phospholipase A2 but also at the level of cyclo-oxygenase/PGE isomerase. Br J Pharmacol. 1989 Dec; 98(4): 1287–1295. doi: 10.1111/j.1476-3811.1989.tb12676.x PMID: PMC1854794 PMID: 2514948
96. Jamie D Croxtall, Qam Choudhury, and Rod J Flower Glucocorticoids act within minutes to inhibit recruitment of signalling factors to activated EGF receptors through a receptor-dependent, transcription-independent mechanism Br J Pharmacol. 2000 May; 130(2): 289–298. doi: 10.1038/sj.bjp.0703272 PMID: PMC1572055 PMID: 10807665

*Autor:

Brogna Carlo M.D.:

Achieved both titles in Medicine (Salerno University Medical school) and Dental School (Pescara University Dental School);

Specialist in oral facial pain (Pescara University Dental School) and expert in oral surgery (few period at NJDS-Usa);

Attended in Neurosurgery (thesis in “The trochlear nerve: microanatomic and endoscopic study” - Salerno University Medical school).

E-mail: c.brogna@libero.it Montemiletto (Av)- Italy.